A Piezoelectric Energy-Harvesting System with Parallel-SSHI Rectifier and Integrated MPPT Achieving 417% Energy-Extraction Improvement and 97% Tracking Efficiency

Shuo Li[1], Abhishek Roy[2], Benton H. Calhoun[1]
[1]University of Virginia, Charlottesville, VA, [2]Marvell Semiconductor, Inc., Marlborough, MA, Email: sl6sf@virginia.edu

Abstract
This work presents an integrated maximum-power-point tracking (MPPT) algorithm and its implementation for the high-performance parallel-synchronized-switch harvesting-on-inductor (SSHI) rectifier, which uses the Perturb and Observe (P&O) method and a proposed power monitor for output power evaluation. Fabricated in 130nm, this piezoelectric energy-harvesting system implements a 417% FOM rectifier with 97% tracking efficiency MPPT, which makes it the first work demonstrating a parallel-SSHI rectifier and high tracking-efficiency MPPT simultaneously.

Introduction

A piezoelectric energy harvester (PEH) extracts the AC energy from mechanical vibrations using different types of rectifiers, like the full-bridge rectifier (FBR) and parallel-SSHI, among which the parallel-SSHI has one of the highest energy-extraction capabilities. Unlike the FBR, whose maximum power-point (MPP) is half of the open-circuit voltage (V_{OC}), the MPP of the parallel-SSHI is related to the PEH characteristics, excitation source, and the flipping efficiency, which makes the fractional-V_{OC} MPPT infeasible. Other MPPT algorithms have also been developed, like P&O [2]. The advantage of P&O is its independence from the harvester characteristics, which makes it very suitable for the parallel-SSHI. The P&O requires output power (P_{OUT}) evaluation, which has been implemented for electrostatic energy harvesters [2] that assume a much higher input voltage than the output. PEHs needs a P_{OUT} evaluation that matches the input voltage level and considers the excitation frequency. This work includes a parallel-SSHI rectifier [3] and proposes a power evaluation method to calculate the P_{OUT} of the piezoelectric harvesting interface, which enables P&O operation and achieves the first effective MPPT for the parallel-SSHI.

MPPT Algorithm

Fig. 2 shows the flow chart of the P&O method used in the MPPT algorithm. First, it compares the current P_{OUT} with the previous P_{OUT} using the proposed power evaluation method. If the current P_{OUT} is larger, V_{REC} will keep the same transition direction as previous, otherwise it will reverse the transition direction. After V_{REC} arrives to a new voltage level, it will wait N−1 switching-cycles of the buck-boost converter (N is programmable from 3 to 6) to become steady state, and then evaluate the next P_{OUT} at the N-th switching pulse. After each power evaluation and comparison, V_{REC} will change to a new voltage level at the next half-vibration-cycle. During the whole MPPT, the P_{OUT} evaluation process affects the tracking efficiency of the MPPT and power consumption of the system. The proposed power evaluation method is based on the switching time of the buck-boost converter. It assumes V_{STORE} keeps constant during the comparison cycle because of the large storage capacitor (4.7mF in this work) and calculates P_{OUT} by dividing the energy during one switching pulse, T_{SWL}, by its corresponding switching cycle, T_{CYC}. A timing diagram in Fig. 2 shows how the P&O method and the proposed P_{OUT} evaluation work to find the MPP of the rectifier.

Implementation

The block diagram of the piezoelectric energy-harvesting system is shown in Fig. 3. The parallel-SSHI adopts the active rectifier (AR) and active diode structure. Transistor M_S is used for the cold start-up of the system. To minimize the off-chip components and system volume, the inductor, $L_{R\text{-}M}$, is shared by the rectifier and the converter through an inductor sharing block. The SW_H control synchronizes the switching of the converter at the falling edge of SW_R, which eliminates the confliction of the inductor sharing and facilitate the design, as shown in Fig. 4. The detailed implementation of each block in the proposed power monitor is shown in Fig. 5. The time-to-voltage converter (TVC) uses a bias current to charge a capacitor, which generates a time-proportional voltage for T_{SWL} and T_{CYC}. Then, the voltage is converted to a nA-current, which flows to two MOSFETs operating in the subthreshold (sub-V_T) region. Due to the exponential relationship of V_{GS} and I_D of the transistor, V_{GS} represents the log value of P_{OUT}. Finally, the calculated P_{OUT} is stored on the capacitor in the S/H block. To minimize the leakage of the capacitor and reduce the power evaluation error, an ultra-low-leakage switch is adopted. The whole MPPT algorithm is implemented in the analog domain eliminating the need of AD/DA and DSP for the digital algorithm, which keeps the power consumption very low. To drive the large capacitor in S/H block while keeping low power, a duty-cycled buffer is adopted. With all these power-reduction techniques, the measured quiescent current of the MPPT is only 0.9μA, which is very power efficient.

Measurement Results

The piezoelectric harvesting system is fabricated in 130nm CMOS. Fig. 6 shows the start-up transient waveform of the whole system. After V_{STORE} is charged up to 3.3V, it is regulated by the on-chip power clamp. The measured rectifier output power shows that the parallel-SSHI can extract a maximum 30.53μW while the on-chip AR can only extract a maximum 6.9μW. The measured maximum power efficiency of the buck-boost converter is 78%. Fig. 7 shows the steady-state transient waveform of the MPPT algorithm, which exactly shows the expected P&O waveform and the evaluated P_{OUT} stored in the S/H block. The measured manually-tuned maximum P_{OUT} and the P_{OUT} with automatic MPPT over V_{OC} and excitation frequency show a tracking efficiency up to 97%. The performance comparison in Fig. 8 shows the parallel-SSHI in this work achieves a 417% FOM, which is 4× higher than the FBRs used with other MPPT algorithms and previous parallel-SSHI rectifiers do not have any MPPTs. Our design implements the first parallel-SSHI rectifier with > 400% FOM and > 90% tracking efficiency MPPT simultaneously.

Acknowledgements

This work is funded in part by NSF (EEC-1160483, 1646454).

References

[1] M. Shim, et al., ISSCC, pp. 406-407, 2014
[2] S. Stanzione, et al., ISSCC, pp. 74-75, 2013
[3] D. A. Sanchez, et al., ISSCC, pp. 366-367, 2016
[4] E. E. Aktakka, et al., JSSC, vol. 49, no. 9, pp. 2017-2029, 2014

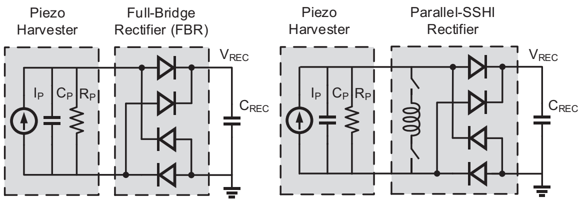

	FBR	Parallel-SSHI
Energy-Extraction Capability	Low	High
Maximum Power Point	1/2·V_{OC}	Related to PEH, excitation, and η_F [3]

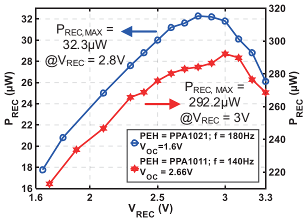

Fig. 1. Characteristics of the FBR and parallel-SSHI and measured MPP of the parallel-SSHI in this work.

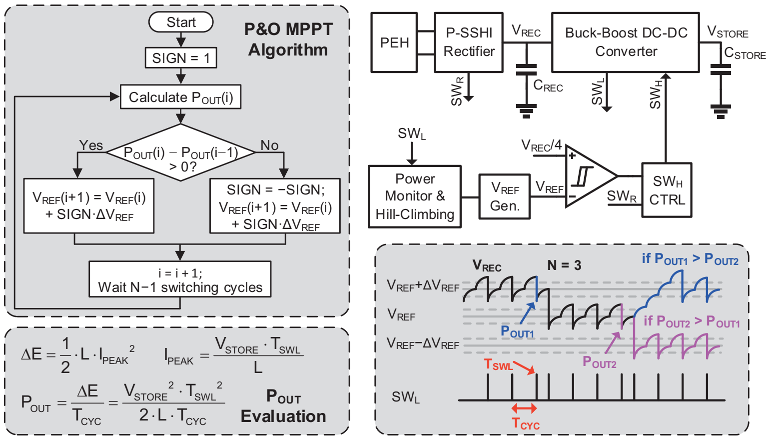

Fig. 2. Flow chart of the MPPT algorithm and its block diagram; the proposed POUT evaluation method and the MPPT operation timing diagram.

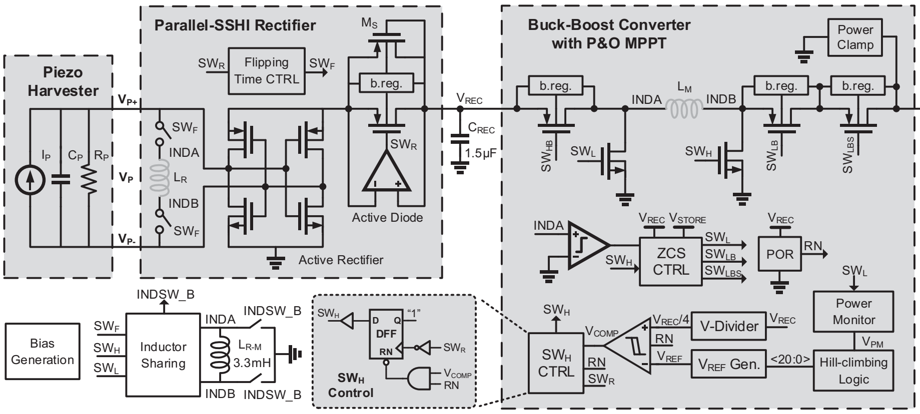

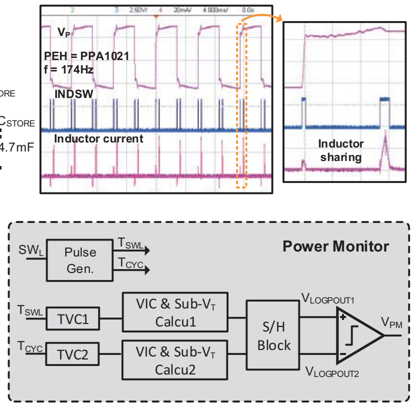

Fig. 3. Block diagram of the piezoelectric energy-harvesting system.

Fig. 4. Measured VP transient waveform and the proposed power monitor block diagram.

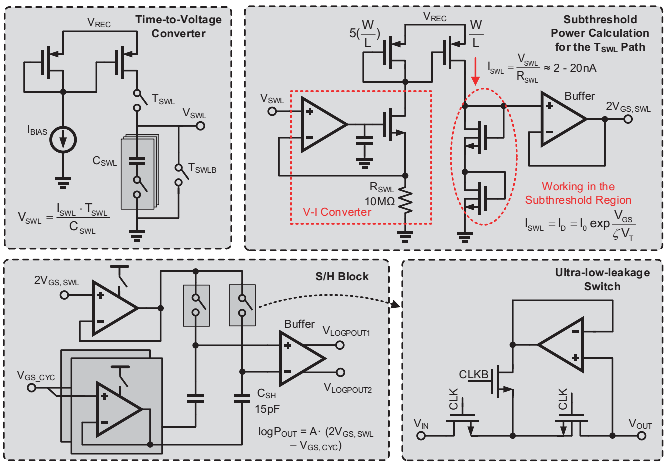

Fig. 5. Implementation of each block in the proposed power monitor, including TVC, subthreshold power calculation and S/H block.

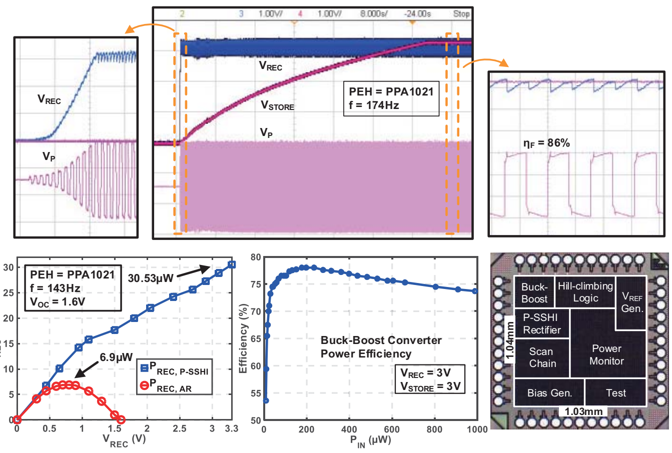

Fig. 6. Measured transient start-up waveform, measured PREC vs. VREC, measured buck-boost converter efficiency, and chip micrograph.

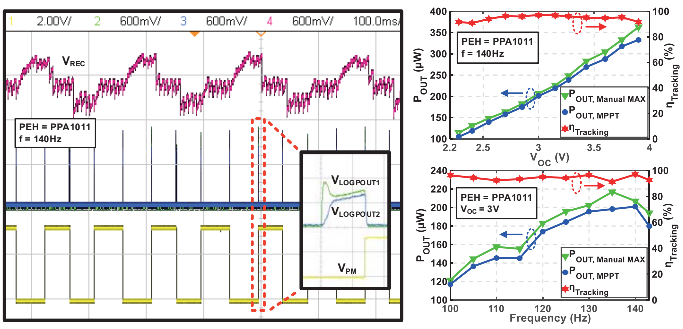

Fig. 7. Measured MPPT steady-state waveform and measured tracking efficiency vs. VOC and excitation frequency.

	This work	[1] ISSCC'14	[2] ISSCC'13	[3] ISSCC'16	[4] JSSC'14
Process	0.13μm	0.35μm	0.25μm	0.35μm	0.18μm
Harvester Type	Piezoelectric	Piezoelectric	Electrostatic	Piezoelectric	Piezoelectric
Piezoelectric Harvester	MIDE PPA1021 & PPA1011	MIDE V20W & V21BL	N/A	MIDE V21B & V22B	Custom MEMS
Harvester Capacitance (nF)	20 & 100	11	N/A	26, 20 & 9	8.5
Rectifier Scheme	Parallel-SSHI	FBR	Off-chip FBR	Parallel-SSHI	Parallel-SSHI
Operation Frequency (Hz)	100 - 180	N/R	N/R	134.6 - 229.2	155 & 419
MPPT	Yes	Yes	Yes	No	No
MPPT Algorithm	P&O	Fractional V_{OC}	VS-P&O	N/A	N/A
Flipping Efficiency	0.86	N/A	N/A	0.93	0.76**
Energy-Extraction Improvement (FOM*)	**417%**	**90%**	**< 100%**	**681%**	**266%****
Maximum MPPT Efficiency	**97%**	**99%**	**99.9%**	**N/A**	**N/A**
Rectifier (>400% FOM) + MPPT (>90% Efficiency)	**Yes**	**No**	**No**	**No**	**No**

N/A = Not Applicable; N/R = Not Reported; * $FOM = P_{REC}/(C_P \cdot V_{OC}^2 \cdot f)$; ** Calculated from the paper

Fig. 8. Comparison with state-of-the-art piezoelectric harvesting interfaces and MPPT algorithms.